The Astrophysical Journal, 604:892–899, 2004 April 1

POSITRON-EMITTER PRODUCTION IN SOLAR FLARES FROM ^{3}He REACTIONS

Benzion Kozlovsky
School of Physics and Astronomy, Tel Aviv University, Ramat Aviv, Tel Aviv 69978, Israel

and

R. J. Murphy and G. H. Share
E. O. Hulburt Center for Space Research, Code 7650, Naval Research Laboratory, Washington, DC 20375
Received 2003 October 2; accepted 2003 December 11

ABSTRACT

We treat in detail positron production from the decay of radioactive nuclei produced in nuclear reactions of accelerated ^{3}He. Because of their large cross sections and low threshold energies, these reactions can significantly contribute to positron production in solar flares with accelerated-particle compositions enriched in ^{3}He. The addition of these ^{3}He reactions extends earlier calculations of positron production by accelerated protons and α-particles. ^{3}He reactions not only add significantly to the total positron yield in flares, but can also yield a positron depth distribution that peaks higher in the solar atmosphere. We discuss the impact these reactions have on the analysis of the annihilation line observed with *RHESSI* from the 2002 July 23 flare. A significant contribution from ^{3}He reactions expands the utility of the annihilation line as a sensitive tool for investigating the structure of the flaring solar atmosphere.

Subject headings: acceleration of particles — nuclear reactions, nucleosynthesis, abundances — Sun: flares — Sun: X-rays, gamma rays

1. INTRODUCTION

In the solar photosphere, the abundance of ^{3}He is believed to be quite small. Although direct spectroscopic measurement of its photospheric abundance is not possible, estimates of the ^{3}He/H ratio derived from solar wind, corona, and meteoritic measurements range from 1.2×10^{-5} (Anders & Grevesse 1989) to 3.4×10^{-5} (Geiss 1982). However, in impulsive solar energetic particle (SEP) events observed in interplanetary space (where the abundances of accelerated particles heavier than oxygen can be enhanced by factors of 3–10), ^{3}He can be enhanced by several orders of magnitude, with ^{3}He/α values of unity or even greater (Reames, Meyer, & von Rosenvinge 1994). While large SEP events are thought to be accelerated by shocks in the solar corona and interplanetary space (Reames 1999, 2000), impulsive SEP events are believed to originate low in the solar atmosphere. Aschwanden et al. (1996) places the height of the impulsive event acceleration region at $(18-20) \times 10^4$ km.

Analyses of gamma-ray line flares (e.g., Murphy, Dermer, & Ramaty 1987; Share & Murphy 1999), which are also believed to occur in the lower solar atmosphere, have shown that the abundances of the heavy accelerated particles responsible for broad gamma-ray lines are also enhanced, possibly in a manner similar to the impulsive SEP event enhancements, suggesting that these two populations may be accelerated by the same process. Observations of gamma-ray lines produced predominantly by accelerated ^{3}He, such as the 0.937 MeV line of ^{18}F from the reaction ^{16}O(^{3}He, p)^{18}F*, can directly measure the ^{3}He abundance. Studies of this line measured by the moderate-resolution *Solar Maximum Mission* (*SMM*) Gamma-Ray Spectrometer (GRS) detectors for several solar flares (Share & Murphy 1998; Mandzhavidze, Ramaty, & Kozlovsky 1997, 1999) have suggested that the ^{3}He/α ratio could be $\sim$0.1 or even larger. If accelerated ^{3}He is significantly enhanced in gamma-ray line flares as these studies suggest, calculations of yields of accelerated-particle reactions must take this into account.

Recent high spectral resolution measurements of the 0.511 MeV positron annihilation line (Share et al. 2003) by *RHESSI* have focused attention on the processes responsible for the formation of this line. Kozlovsky, Lingenfelter, & Ramaty (1987) provided a detailed treatment of positron production from the decay of radioactive nuclei produced in nuclear interactions of accelerated protons and α-particles with the most abundant ambient elements. A computer code to calculate the yields for various accelerated particle spectra and interaction models was constructed using the cross sections given in that paper. The code has been used in many investigations (e.g., Murphy et al. 1987) concerning the observation of the 0.511 MeV annihilation line produced when the positrons annihilate with ambient electrons.

In this paper, we extend the calculations of Kozlovsky et al. (1987) to include the most important positron-emitter–producing reactions of accelerated ^{3}He. These ^{3}He reactions are important because of their very low threshold energies and large cross sections at low energies. As a result of the low threshold energies, these reactions may dominate positron-emitter production for steep accelerated-particle spectra when the accelerated particles are enriched with ^{3}He. As we show, the reactions not only add significantly to the total positron-production yields but can also affect the depth distribution of positron-emitter production in the solar atmosphere. The inclusion of ^{3}He reactions is critical to ensure the accuracy of the positron annihilation line as a sensitive tool for investigating both the flare acceleration process and the structure of the flaring solar atmosphere. We discuss the impact these reactions have on the analysis (Share et al. 2003) of the annihilation line observed with *RHESSI* from the 2002 July 23 flare, for which two very different scenarios have been suggested to explain the observed line profile.

Report Documentation Page

Form Approved
OMB No. 0704-0188

1. REPORT DATE	2. REPORT TYPE	3. DATES COVERED
01 APR 2004		**00-00-2004 to 00-00-2004**

4. TITLE AND SUBTITLE	5a. CONTRACT NUMBER
Positron-Emitter Production in Solar Flares from 3He Reactions	5b. GRANT NUMBER
	5c. PROGRAM ELEMENT NUMBER
6. AUTHOR(S)	5d. PROJECT NUMBER
	5e. TASK NUMBER
	5f. WORK UNIT NUMBER
7. PERFORMING ORGANIZATION NAME(S) AND ADDRESS(ES) **Naval Research Laboratory,E. O. Hulburt Center for Space Research,4555 Overlook Avenue, SW,Washington,DC,20375**	8. PERFORMING ORGANIZATION REPORT NUMBER
9. SPONSORING/MONITORING AGENCY NAME(S) AND ADDRESS(ES)	10. SPONSOR/MONITOR'S ACRONYM(S)
	11. SPONSOR/MONITOR'S REPORT NUMBER(S)

12. DISTRIBUTION/AVAILABILITY STATEMENT
Approved for public release; distribution unlimited

13. SUPPLEMENTARY NOTES

14. ABSTRACT

We treat in detail positron production from the decay of radioactive nuclei produced in nuclear reactions of accelerated 3He. Because of their large cross sections and low threshold energies, these reactions can significantly contribute to positron production in solar flares with accelerated-particle compositions enriched in 3He. The addition of these 3He reactions extends earlier calculations of positron production by accelerated protons and -particles. 3He reactions not only add significantly to the total positron yield in flares, but can also yield a positron depth distribution that peaks higher in the solar atmosphere. We discuss the impact these reactions have on the analysis of the annihilation line observed with RHESSI from the 2002 July 23 flare. A significant contribution from 3He reactions expands the utility of the annihilation line as a sensitive tool for investigating the structure of the flaring solar atmosphere.

15. SUBJECT TERMS

16. SECURITY CLASSIFICATION OF:			17. LIMITATION OF ABSTRACT	18. NUMBER OF PAGES	19a. NAME OF RESPONSIBLE PERSON
a. REPORT **unclassified**	b. ABSTRACT **unclassified**	c. THIS PAGE **unclassified**	**Same as Report (SAR)**	**8**	

TABLE 1
^{3}He-Induced Reaction Products and Threshold Energies (MeV nucleon^{-1})

Target	Products			
	n	p	"d"[a]	"α"[b]
^{12}C.....	^{14}O (0.49)[c]	^{14}N (0)	^{13}N (1.48)[c]	^{11}C (0)[c]
^{14}N.....	^{16}F (0.47)[c]	^{16}O (0)	^{15}O (0)[c]	^{13}N (0)[c]
^{16}O.....	^{18}Ne (1.17)[c]	^{18}F (0)[c]	^{17}F (1.94)[c]	^{15}O (0)[c]
^{20}Ne.....	^{22}Mg (0)[c]	^{22}N (0)[c]	^{21}N (1.17)[c]	^{19}Ne (0)[c]
^{24}Mg.....	^{26}Si (0.024)[c]	^{26}Al (0)[c]	^{25}Al (1.21)[c]	^{23}Mg (0)[c]
^{28}Si.....	^{30}S (0.165)[c]	^{30}P (0)[c]	^{29}P (1.02)[c]	^{27}Si (0)[c]
^{56}Fe.....	^{58}Ni (0)	^{58}Co (0)[c]	^{57}Co (0)	^{55}Fe (0)

Note.—Threshold energies are given in parentheses.
[a] "d" denotes either d or p, n.
[b] "α" denotes either α or various combinations of nucleons.
[c] Radioactive positron emitter.

In § 2 we present the cross sections for positron-emitter production by accelerated ^{3}He. In § 3 we calculate positron yields for various accelerated particle spectra, and in § 4 we relate the results to the annihilation-line measurements of the 2002 July 23 flare observed by *RHESSI*.

2. CROSS SECTIONS

In Table 1, we list the products and corresponding threshold energies (shown in parentheses) of the most important ^{3}He reactions with the most abundant elements in the solar atmosphere. (A value of 0 indicates an exothermic reaction.) Conspicuous features of this table are that most of the reactions are exothermic and that the endothermic reactions have very low threshold energies. The reason for these uniquely low thresholds is the high mass excess of ^{3}He (15.8 MeV). This excess is also responsible for highly excited compound systems in these reactions and hence for their large cross sections. These characteristics are the reason that ^{3}He-induced reactions have marked advantages for nuclear research when only low-energy accelerators (less than 5 MeV) are available (e.g., Bromley & Almqvist 1960). Most of the products shown in Table 1 are radioactive positron-emitting nuclei. (The radioactive products of Fe reactions mostly decay via electron capture.) Furthermore, most of these products have short lifetimes (see Kozlovsky et al. 1987 for a list of lifetimes) and hence can contribute to the observed 0.511 MeV positron-annihilation line in solar flares, for which observation times are typically tens of minutes. Kozlovsky et al. (1987) found these same radioactive nuclei to be the most important contributors to positron production by accelerated protons and α-particles in solar flares.

In the following sections, we discuss the cross sections for production of radioactive positron-emitters by ^{3}He reactions with the various target nuclei of Table 1. In Figures 1–6 we show the estimated cross sections of the various reactions for the energy range of 1–100 MeV nucleon^{-1}. We discuss the large body of laboratory cross section measurements that we use, but these measurements do not always cover the full energy range. We use the following rules, based on extensive studies, to estimate cross sections for which measurements are not available.

1. For reactions whose exit channel contains multiple particles of the form (^{3}He, *kpln*), where k and l are integers and $k, l \geq 2$, the structure of the cross section consists of a steep rise from threshold energy to a first peak, followed by a minimum, and then a second rise to a flat plateau. The first peak is due to emission of an α-particle (mainly via a compound mechanism), and the plateau is due to emission of progressively more and more nucleons (e.g., Gadioli & Hodgson 1986; Michel & Galas 1983).

2. For reactions whose exit channel contains one particle or multiple particles of the form (^{3}He, *kpln*) but where $k, l < 2$ (e.g., ^{3}He, *pn*), the cross sections typically rise steeply from threshold energy to a maximum and then fall rapidly to a long tail.

3. The steep rise of the cross section just above threshold energy to the first maximum is typical of reactions between charged nuclei and represents the penetration factor of the Coulomb barrier (Blatt & Weisskopf 1952). This behavior can be clearly seen in the numerous measured cross sections compiled by Keller et al. (1973).

4. For a few reactions there were no laboratory measurements available to us. For these reactions, we have estimated the cross sections using the procedure given by Keller, Lange, & Munzel (1974, hereafter KLM74). Based on ~1800 experimentally determined cross sections (compiled by Keller et al. 1973), KLM74 have devised an elaborate semi-empirical procedure for obtaining estimates of unknown cross sections for accelerated p, d, ^{3}He, and α reactions with nuclei heavier than fluorine.

2.1. *Reactions of* ^{3}He *with* ^{12}C

The radioactive positron-emitting nuclei produced in ^{3}He reactions with ^{12}C are ^{14}O, ^{13}N, and ^{11}C, as shown in Table 1. In Figure 1, we present the cross sections for these reactions. The data from 2 to 8 MeV nucleon^{-1} are from Cochran & Knight (1962), from 0.6 to 3.3 MeV nucleon^{-1} from Hahn & Ricci (1966), and from 1.6 to 11 MeV nucleon^{-1} from Brill (1965). At higher energies the cross section for ^{11}C is from Crandall et al. (1956) and Aslanides et al. (1981). The laboratory measurements of the cross section for production of ^{11}C, which cover the entire energy range of interest here, clearly demonstrate the validity of rule 1 above.

2.2. *Reactions of* ^{3}He *with* ^{14}N

The radioactive positron-emitting nuclei produced in ^{3}He reactions with ^{14}N are ^{16}F, ^{15}O, and ^{13}N, as shown in Table 1. In Figure 2, we present the cross sections for these reactions.

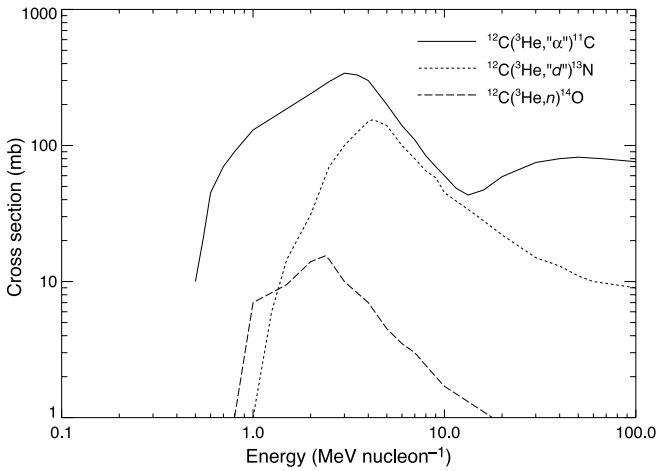

Fig. 1.—Radioactive positron-emitter production cross sections for ^{3}He reactions on ^{12}C.

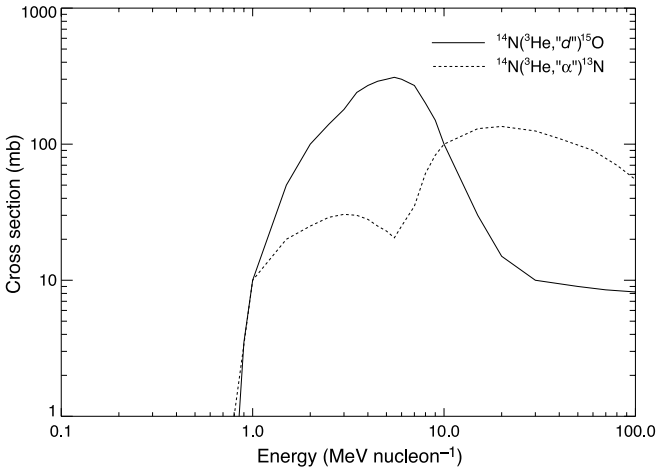

FIG. 2.—Radioactive positron-emitter production cross sections for ^{3}He reactions on ^{14}N.

The data for ^{15}O from 2 to 6 MeV nucleon^{-1} are from Hahn & Ricci (1967). At higher energies, we followed the anticipated behavior for this kind of reaction according to the above rules. For ^{13}N, we use the data from Hahn & Ricci (1966) at ~0.6 MeV nucleon^{-1} and from Brill (1965) at 3.3–10 MeV nucleon^{-1}. Here we again confirm the rule concerning the rise of the cross section. The higher energy rise begins just beyond the threshold for the (^{3}He, ^{3}Hen) reaction and is consistent with the explanation that the rise is due to the emission of several particles in the exit channel rather than α only.

The cross section for production of ^{16}F is not available, but the (^{3}He, n) reaction is almost always the weakest of the reactions in Table 1 and always much less than the (^{3}He, α) reaction. We therefore estimate that the cross section for ^{16}F will be much less than 30 mbarn, which is the value of the first maximum for the (^{3}He, α) reaction (see Fig. 2), so we do not include it here.

2.3. *Reactions of* ^{3}He *with* ^{16}O

The radioactive positron-emitting nuclei produced in ^{3}He reactions with ^{16}O are ^{18}Ne, ^{18}F, ^{17}F, and ^{15}O, as shown in Table 1. In Figure 3, we present the cross sections for these reactions. The cross section for ^{18}Ne from 1.3 to 13 MeV nucleon^{-1} is based on the cross section measurements by Tatischeff et al. (2003) for the reaction ^{16}O(^{3}He, $n\gamma_{1.887}$)^{18}Ne. We have multiplied this cross section by 1.5 to account for additional ^{18}Ne production in the ground state and in other levels that decay directly to the ground state. The data for ^{18}F from 0.9 to 3.2 MeV nucleon^{-1} are from Hahn & Ricci (1966); from 4.3 to 13.3 MeV nucleon^{-1} they are from Fitschen et al. (1977). This cross section includes the production of ^{18}F via the decay of ^{18}Ne. The data for ^{15}O from 0.9 to 3.2 MeV nucleon^{-1} are from Hahn & Ricci (1966). We obtained a cross section value at 7 MeV nucleon^{-1} from the evaluation by Brill (1965) and at 8 MeV nucleon^{-1} by integrating the angular-dependent cross sections of Fuchs & Oeschler 1973). We constructed the complete cross section according to the rules discussed above. The data for ^{17}F are from Hahn & Ricci (1966) for 2.5–3 MeV nucleon^{-1}. Again, we constructed the complete cross section according to the rules discussed above.

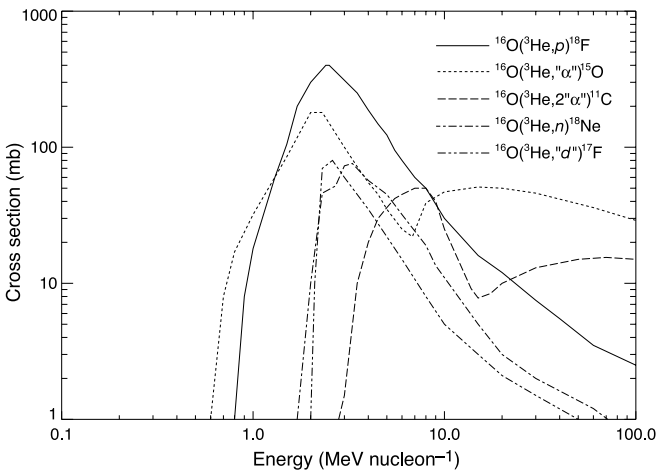

FIG. 3.—Radioactive positron-emitter production cross sections for ^{3}He reactions on ^{16}O.

In addition to the above reactions from Table 1, we also show in Figure 3 the cross section for the reaction producing ^{11}C from the reaction (^{3}He, 2α). The data from 3.6 to 10 MeV nucleon^{-1} are from Brill (1965). At higher energies we constructed the cross section according to the above rules with a rise to a plateau.

2.4. *Reactions of* ^{3}He *with* ^{20}Ne

All of the reaction products of ^{3}He reactions with ^{20}Ne shown in Table 1 are radioactive positron-emitting nuclei. Because the half-life of ^{22}Na is so long (2.6 yr), we do not consider it here. Since the total cross sections for the remaining nuclei are not available in the literature, we estimated them by using the procedure given by KLM74. The resulting cross sections were identical to cross sections of the corresponding reactions of ^{3}He with ^{24}Mg, when estimated by the same procedure. We therefore use the measured ^{24}Mg cross sections for the n, p, d, and α reactions of Table 1 for the corresponding ^{20}Ne reactions. The ^{24}Mg cross sections are discussed in the next section.

2.5. *Reactions of* ^{3}He *with* ^{24}Mg

The radioactive positron-emitting nuclei produced in ^{3}He reactions with ^{24}Mg are ^{26}Si, ^{26}Al, ^{25}Al, and ^{23}Mg, as listed in Table 1. In Figure 4, we present their cross sections. The data

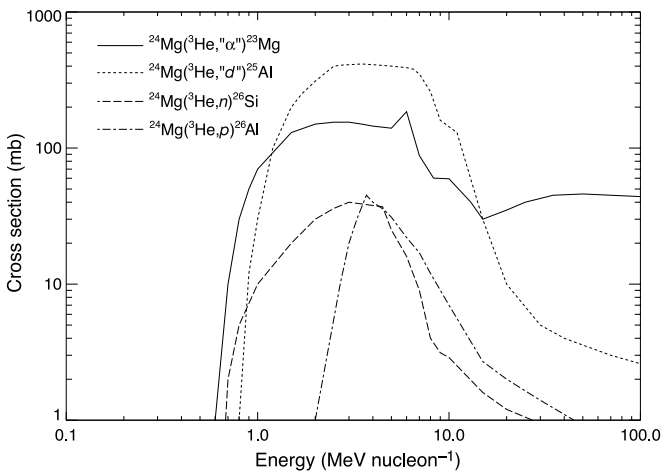

FIG. 4.—Radioactive positron-emitter production cross sections for ^{3}He reactions on ^{24}Mg. These cross sections are also used as the cross sections for the corresponding n, p, d, and α reactions of ^{20}Ne.

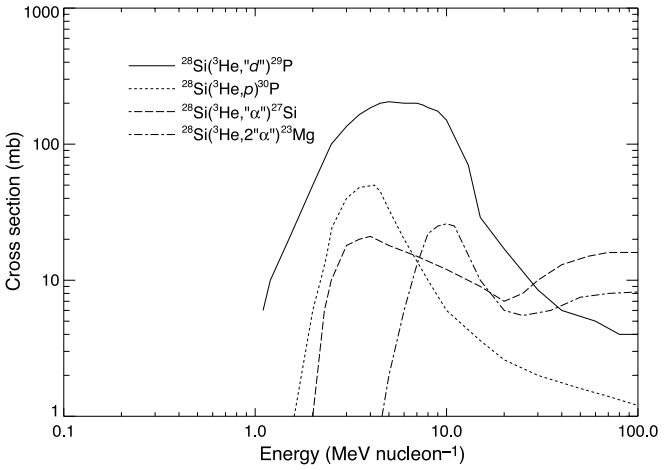

FIG. 5.—Radioactive positron-emitter production cross sections for ^{3}He reactions on ^{28}Si.

for ^{26}Si, ^{25}Al, and ^{23}Mg from 3.6 to 13.3 MeV nucleon^{-1} are from Frantzvog et al. (1982). At energies less than 3.6 MeV nucleon^{-1} and greater than 13.3 MeV nucleon^{-1}, we constructed the complete cross sections according to the rules discussed above. For ^{26}Al, we constructed the cross section according to the procedure given by KLM74. We assume that 50% of the total cross section produces the radioactive positron-emitter ^{26m}Al.

2.6. *Reactions of* ^{3}He *with* ^{28}Si

The radioactive positron-emitting nuclei produced in ^{3}He reactions with ^{28}Si are ^{30}S, ^{30}P, ^{29}P, and ^{27}Si. These reactions are listed in Table 1, and in Figure 5 we show their cross sections. The data for ^{29}P from 3.6 to 13.3 MeV nucleon^{-1} are from Frantzvog et al. (1982). For ^{30}P and ^{27}Si, we constructed the cross section according to the procedure given by KLM74. According to KLM74, the cross section for producing ^{30}S is less than 10 mbarn, so we do not include it here.

In addition to the above reactions from Table 1, we also show in Figure 5 the cross section for the reaction producing ^{23}Mg from the reaction (^{3}He, 2α). The data from 3.6 to 13.3 MeV nucleon^{-1} are from Frantzvog et al. (1982). At higher energies, we constructed the cross section according to the above rules, with a rise to a plateau.

2.7. *Reactions of* ^{3}He *with* ^{56}Fe

The only radioactive positron-emitting nucleus produced in ^{3}He reactions with ^{56}Fe shown in Table 1 is ^{58}Co, in which only 15% of the decays emit a positron. ^{55}Fe and ^{57}Co decay only by electron capture. Since the cross section for total ^{58}Co production is less than 50 mbarn (Hazan & Blann 1965), we do not include it here.

In addition to the reactions in Table 1, we consider production of ^{56}Co and ^{57}Ni. A total of 20% of ^{56}Co and 47% of ^{57}Ni decay via positron emission. We show in Figure 6 the cross sections for the production of ^{56}Co and ^{57}Ni; the data from 2 to 10 MeV nucleon^{-1} are from Hazan & Blann (1965).

3. POSITRON YIELDS

We calculate thick-target positron yields from accelerated proton, ^{3}He and α-particle reactions according to the formalism given in Ramaty (1986). The ambient and accelerated-ion abundances used in the calculations are summarized in Table 2. For the ambient medium we have assumed coronal abundances (Reames 1995) for C, N, O, Mg, Al, Si, S, Ca, and Fe relative to H and have taken Ne/O = 0.25, He/H = 0.10, and ^{3}He/H $= 3 \times 10^{-5}$. These are the same ambient abundances used by Ramaty, Mandzhavidze, & Kozlovsky (1996), except for He/H, for which they assumed the coronal value of 0.037. We assume various values for accelerated ^{3}He/α, and for the other accelerated ions we assume "impulsive flare" abundances defined by Ramaty et al. (1996), which are coronal (Reames 1995) for C, N, Ne, Mg, Al, Si, S, Ca, and Fe relative to O but have Ne/O, Mg/O, Si/O and S/O ratios increased by a factor of 3, Fe/O increased by a factor of 10, and α/O = 50. This composition reflects average heavy-element abundance enhancements found in impulsive SEP events in space (Reames et al. 1994). We also assume $\alpha/p = 0.5$, which is at the maximum of the range observed in impulsive SEP events. Analyses of gamma-ray line flares (Share & Murphy 1997; Mandzhavidze et al. 1997, 1999) have suggested that the large observed flux of the α-α line complex at $\sim$0.47 MeV requires either such a large value of accelerated α/p or a correspondingly large value of ambient ^{4}He/H, which is probably less likely. We assume a power-law form for the energy spectra of the accelerated ions, normalized so that the number of accelerated protons greater than 10 MeV is 1, and we assume that all species have the same spectral index. For the proton and α-particle reactions, we use the cross sections given by Kozlovsky et al. (1987), which include the pion-producing reactions.

In Figure 7, we show total thick-target positron yields, Q_+, as functions of the accelerated-particle power law spectral index s for accelerated ^{3}He/α ratios of 0, 0.1, 0.5, and 1. For harder spectra ($s < \sim 3$), the ^{3}He contribution is negligible even for He/$\alpha = 13$, with positron production being primarily from accelerated protons and α particles (for the hardest spectra, positrons from the decay of pions produced by accelerated protons are most important). For steeper spectra ($s > \sim 3$), the contribution from ^{3}He can dominate (at $s = 5.5$ and He/$\alpha = 13$, the increase is about an order of magnitude). We note that even the yields calculated here for He/$\alpha = 13$ (when renormalized to 1 proton >30 MeV) are larger than those calculated by Kozlovsky et al. (1987), except for the hardest spectra, where the production is primarily from the decay of pions from proton

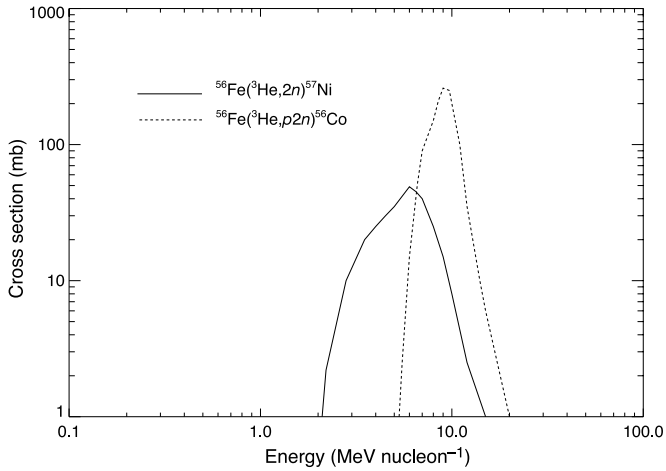

FIG. 6.—Radioactive positron-emitter production cross sections for ^{3}He reactions on ^{56}Fe.

TABLE 2
AMBIENT AND ACCELERATED-ION COMPOSITIONS

Element	Ambient	Accelerated
H	1.0	1.0
^{3}He	3.0×10^{-5}	[a]
^{4}He	0.1	0.5
C	2.96×10^{-4}	4.65×10^{-3}
N	7.90×10^{-5}	1.24×10^{-3}
O	6.37×10^{-4}	1.00×10^{-2}
Ne	1.59×10^{-4}	4.55×10^{-3}
Mg	1.25×10^{-4}	5.89×10^{-3}
Al	1.00×10^{-5}	1.57×10^{-4}
Si	9.68×10^{-5}	4.55×10^{-3}
S	2.03×10^{-5}	9.56×10^{-4}
Ca	6.75×10^{-6}	1.06×10^{-4}
Fe	8.54×10^{-5}	1.34×10^{-2}

[a] The calculations are performed for various values of the accelerated ^{3}He abundance.

interactions. This increase is due to the different abundances assumed here.

Once emitted, positrons either slow down and annihilate with ambient electrons to produce annihilation photons or escape from the region without significant annihilation during typical solar-flare observation times. Positrons annihilate either directly with ambient electrons (forming two 0.511 MeV photons in the center of mass) or by first forming positronium. Positronium is formed in one of two states depending on the relative spins of the positron and electron: a singlet state (25% of the time) and a triplet state (75% of the time). Annihilation from the singlet state produces two 0.511 MeV photons in the center of mass, while annihilation from the triplet state produces three photons with energies less than 0.511 MeV.

Relevant quantities associated with positron annihilation are (1) the number of 0.511 MeV line photons produced per positron (f_{511}), (2) the fraction of positrons that annihilate via positronium (f_{ps}), and (3) the ratio of the number of photons in the three-photon continuum to the number in the line ($3\gamma/2\gamma$). If the positronium is undisturbed, its annihilation proceeds according to the above percentages so that $f_{511} = 2-1.5f_{ps}$ and $3\gamma/2\gamma = 2.25f_{ps}/(2-1.5f_{ps})$. However, high density or high temperature can quench the longer-lived triplet state, either by ionizing the positronium or by transforming the triplet state to the singlet state by spin flipping. This will tend to increase f_{511} and decrease $3\gamma/2\gamma$. If all of the triplet state is quenched (or if $f_{ps} = 0$), f_{511} will have its maximum value of 2 and $3\gamma/2\gamma = 0$. If $f_{ps} = 1$ and the positronium is undisturbed, f_{511} will be 0.5 and $3\gamma/2\gamma = 4.5$. Care must be taken interpreting measured values of these quantities, since f_{511} can appear reduced and $3\gamma/2\gamma$ modified because of (1) finite observation times (since not all of the emitters can decay to produce positrons and subsequent annihilation photons due to the lifetimes of the various positron emitters), and (2) escape of positrons from the annihilation region.

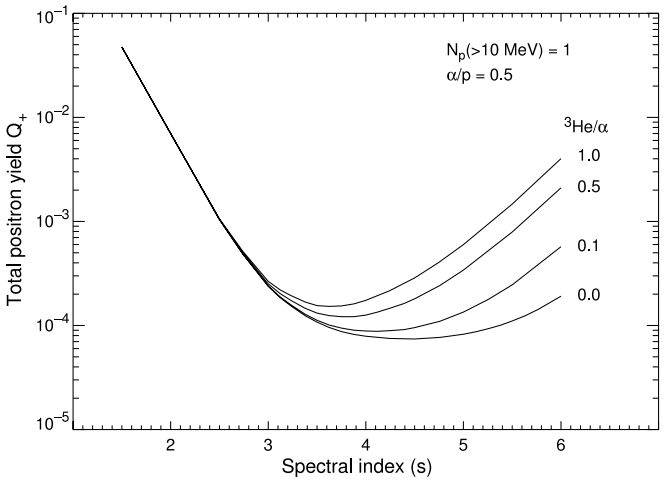

FIG. 7.—Total thick-target positron yield, Q_+, as a function of the accelerated-particle spectral index for $^3\mathrm{He}/\alpha = 0$, 0.1, 0.5, and 1.0.

The lower curves of Figure 8 show calculated ratios of the total 0.511 MeV positron-annihilation line fluence to the summed fluences of the 4.44 and 6.13 MeV ^{12}C and ^{16}O deexcitation lines, as functions of the accelerated particle spectra index s for $^3\mathrm{He}/\alpha = 0$, 0.1, 0.5, and 1.0. We assume a positron to annihilation-line photon conversion factor $f_{511} = 1.0$. If all positrons annihilate within the flare observation time and there is no quenching of the positronium triplet state, this factor would correspond to a positronium fraction of 0.67 and a $3\gamma/2\gamma$ ratio of 1.5. The upper curve of Figure 8 shows the fraction of the total number of annihilation photons observable within the first 1000 s for instantaneous emitter production at $t = 0$, as a function of the accelerated particle spectral index s. For very hard spectra ($s < 3$), positrons are produced primarily via the decay of pions, which have a very short lifetime ($<10^{-5}$ s), and nearly all of the photons are observable. As the spectrum softens, positron production shifts to radioactive emitters with longer lifetimes, and fewer photons are observable. For indices larger than 5 there is a small dependence of this fraction on $^3\mathrm{He}/\alpha$, but the deviation from the shown curve is less than 7% at $s = 6$.

In the next section we compare our calculations of annihilation line yields with measured fluences obtained with *RHESSI* from the 2002 July 23 flare. We also explore the

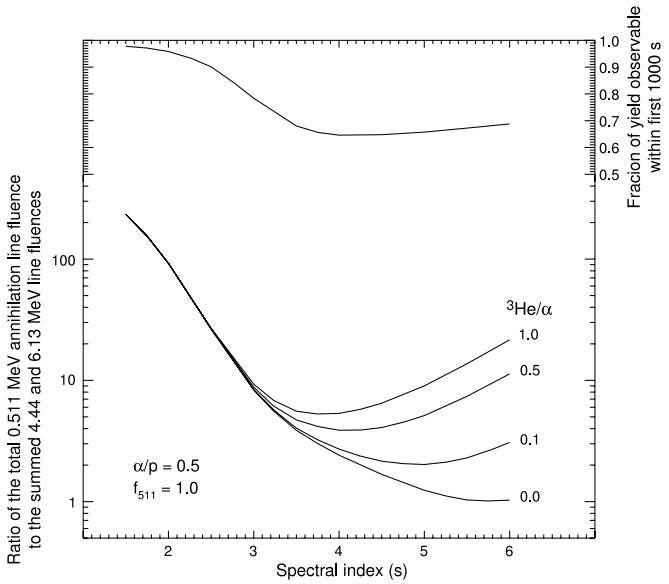

FIG. 8.—*Lower curves*: Calculated ratio of the total 0.511 MeV positron-annihilation line fluence to the summed fluences of the 4.44 and 6.13 MeV ^{12}C and ^{16}O deexcitation lines, as a function of accelerated-particle spectra index s for $^3\mathrm{He}/\alpha = 0$, 0.1, 0.5, and 1.0. The positron to annihilation-line photon conversion factor $f_{511} = 1.0$. *Upper curve*: Fraction of the total positron annihilation photons observable within the first 1000 s, as a function of the accelerated-particle spectral index.

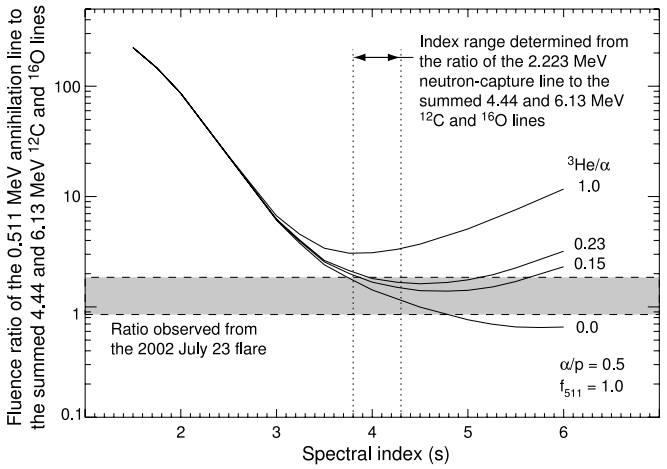

FIG. 9.—Calculated ratio of the 0.511 MeV positron-annihilation line fluence to the summed fluences of the 4.44 and 6.13 MeV ^{12}C and ^{16}O deexcitation lines as a function of the accelerated-particle spectra index s for $^3\mathrm{He}/\alpha = 0$, 0.15, 0.23, and 1.0. The assumed positron to annihilation-line photon conversion factor f_{511} is 1.0, and all curves have been reduced to account for the fraction of the total annihilation-line fluence observable during the 23 July flare observation interval. The $^3\mathrm{He}/\alpha$ values of 0.15 and 0.23 are the 90% and 99% confidence upper limits, respectively, determined from the measured ratio of the 0.937 MeV ^{18}F line fluence upper limit and the $\sim$0.45 MeV α-α complex fluence. The horizontal band indicates the ratio ($\pm 1\ \sigma$) observed by *RHESSI* from the 2002 July 23 flare. The vertical dotted lines indicate the allowed range ($\pm 1\ \sigma$) of spectral index derived from the observed fluence ratio of the 2.223 MeV neutron-capture line to the summed 4.44 and 6.13 MeV ^{12}C and ^{16}O deexcitation lines.

consequences of these calculations for the high spectral resolution measurements of the annihilation line shape.

4. APPLICATION TO THE 2002 JULY 23 SOLAR FLARE

Figure 9 shows calculated ratios of the 0.511 MeV annihilation-line fluence to the summed 4.44 MeV ^{12}C and 6.13 MeV ^{16}O deexcitation-line fluences, as functions of the accelerated-particle spectral index s for the extreme cases of $^3\mathrm{He}/\alpha = 0$ and 1.0. We have taken into account the fraction of the annihilation-line fluence expected to be observed during the 960 s observation time of the July 23 flare, assuming that the positron-emitter–production time history is identical to the nuclear line-emission time history for this flare (Share et al. 2003). Upper limits for the accelerated $^3\mathrm{He}/\alpha$ abundance ratio for this flare, obtained from a comparison of the measured upper limits for the ^{3}He-produced 0.937 MeV line fluence and the fluence of the α-α complex, are 0.15 with 90% confidence and 0.23 with 99% confidence. These values are comparable to the *SMM* 19-flare average for $^3\mathrm{He}/\alpha$ of 0.1 (Share & Murphy 1998). Calculated fluence ratios for these values of $^3\mathrm{He}/\alpha$ are also shown in Figure 9. For all of the curves of Figure 9, f_{511} was assumed to be 1, which corresponds to a positronium fraction f_{ps} of 0.67 and a $3\gamma/2\gamma$ ratio of 1.5. This value for $3\gamma/2\gamma$ is consistent with the measured 99% confidence upper limit of 3.3 (Share et al. 2003). We note that there is some dependency of the calculated ratio on the assumed accelerated α/p abundance ratio. An estimate of this abundance ratio for the 23 July flare can be obtained by comparing calculated fluence ratios of the α-α complex and the summed 4.44 and 6.13 MeV lines with the measured ratio of 2.2 ± 0.9 (Share et al. 2003; Smith et al. 2003). The measured ratio provides a 1 σ lower limit of $\sim$0.35, which is consistent with our assumed value of 0.5.

Also shown in Figure 9 is the measured line ratio for this flare, 1.35 ± 0.5 (Share et al. 2003; Smith et al. 2003), indicated by dashed lines. The vertical dotted lines indicate the range of spectral index deduced (2004, in preparation) from the measured ratio of the 2.223 MeV neutron-capture line fluence to the summed fluences of the 4.44 MeV ^{12}C and 6.13 MeV ^{16}O lines. The calculated line ratio is consistent with the measured ratio for $^3\mathrm{He}/\alpha$ ratios up to at least the 99% confidence value of 0.23. We note that if the α/p ratio were as low as 0.1, the curves of Figures 8 and 10 in the spectral range of interest would be reduced to about 70% of their values for $\alpha/p = 0.5$, and the curves for $^3\mathrm{He}/\alpha$ ratios up to 0.23 would still be consistent with the measured line-fluence ratio. We also note that even if as many as 50% of the positrons were to escape from the region without appreciable annihilation during the observation time, the calculated ratio for $^3\mathrm{He}/\alpha = 0.23$ would still be consistent with the measurement.

The *RHESSI* high-resolution Ge detectors resolved the 0.511 MeV positron-annihilation line observed in the 2002 July 23 solar flare (Share et al. 2003). When fit with a Gaussian line shape, the line was found to be broad with a full width at half maximum (FWHM) of 8.1 ± 1.1 keV. Share et al. (2003) found that the line shape was consistent with two very different production scenarios. The line could have been formed in a quiet solar atmosphere at a temperature of $\sim$6000 K. Under these conditions, the line is composed of both a narrow and a broad component. The narrow component ($\sim$1.5 keV) is produced by annihilation of thermalized positrons with bound electrons, while the broad component ($\sim$7 keV) results from positronium formation by charge exchange in flight with hydrogen. For a narrow range of temperatures, the broad component is sufficiently strong to produce an effective "broad" line. Alternatively, the line could be a thermally broadened Gaussian, whose width corresponds to a temperature of $(4-7) \times 10^5$ K.

Both of these scenarios present difficulties. The difficulty with the first scenario is that it requires an exceptionally fine

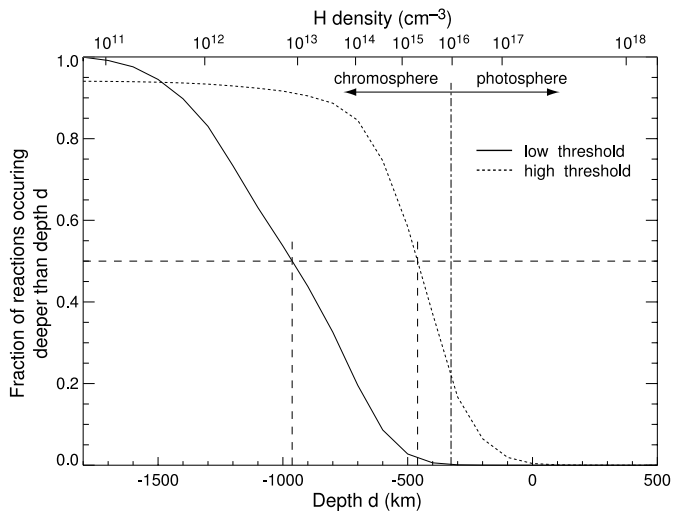

FIG. 10.—Fraction of production occurring deeper than a given depth for two reactions whose cross sections have a low-energy threshold (1 MeV nucleon^{-1}, *solid line*) and a high-energy threshold (25 MeV nucleon^{-1}, *dotted line*). The dashed lines indicate the 50% points on each curve. The assumed atmospheric model is Avrett (1981). The bottom axis is depth in the atmosphere (km) and the top axis is the corresponding hydrogen number density (cm^{-3}).

tuning of the annihilation region, since only for a very narrow range of temperatures (approximately 5650–6270 K) is the broad component sufficiently strong to produce an acceptable fit to the line shape. At temperatures immediately above and below this range, the line becomes very narrow. For the second scenario, calculations (Hua, Ramaty, & Lingenfelter 1989) for a relatively hard accelerated-particle spectrum have shown that the interaction site of nuclear reactions similar to those responsible for positron-emitter production by protons and α-particles is expected to be at hydrogen densities of 10^{14} to 10^{15} cm^{-3}. Current models of the solar atmosphere indicate that the temperature at such high densities is much less than $(4-7)\times10^5$ K.

The new reactions of positron-emitter production by accelerated ^{3}He presented here may help make the second scenario more plausible. The solar atmosphere during flares is known to be significantly altered from quiet-Sun conditions by processes such as heating and mass motion. There is evidence for high temperatures at high densities, for example, in the dramatic enhancement over quiet-Sun values of C IV and Si IV line emission in the transition region, as noted by Brekke et al. (1996). As another example, Raymond et al. (2003) observed large emission measures of 10^5 K gas during the 2002 July 23 flare. Although temperatures as high as $(4-7)\times10^5$ K at the high densities 10^{14}–10^{15} cm^{-3} are still unlikely, if a significant fraction of the positrons were formed at substantially lower densities, as will be shown below, the high temperatures implied by the annihilation line width would be much more plausible there.

As discussed above, the ^{3}He reactions are unique in that their cross sections are both large and have very low threshold energies compared with corresponding proton– and α-particle–induced reactions. For a power-law spectrum of accelerated particles losing energy in an ambient medium, such low-threshold reactions are produced predominantly by particles with low initial energies. These particles have shorter ranges than higher energy particles, so the reactions tend to occur at higher elevations (lower densities) as the particles are moving downward in the solar atmosphere. We demonstrate this by calculating the depth distribution of nuclear reactions having a low threshold energy ($\sim$1 MeV nucleon^{-1}, similar to those of typical positron-emitter reactions by accelerated ^{3}He) and nuclear reactions having a high threshold energy ($\sim$25 MeV nucleon^{-1}, similar to those of typical positron-emitter spallation reactions by accelerated protons).

To perform these calculations, we use the loop model of Hua et al. (1989), which we briefly describe. The model includes energy losses due to Coulomb collisions, removal by nuclear reactions, magnetic mirroring in the convergent flux tube, and MHD pitch-angle scattering (PAS) in the corona (see Hua et al. 1989 for details). The accelerated ions are released isotropically at the top of a magnetic loop and are followed until they interact or thermalize, usually near the loop footpoints in the chromosphere or upper photosphere. The model consists of a semicircular coronal portion and two straight portions extending vertically from the transition region through the chromosphere into the photosphere. Below the transition region, the magnetic-field strength is assumed proportional to a power δ of the pressure (Zweibel & Haber 1983). PAS can be characterized by its mean free path for isotropization, Λ, here expressed by λ, the ratio of Λ to the loop half-length. The level of PAS directly affects the angular distribution of the accelerated particles when they interact with the solar atmosphere. Using gamma-ray line data from several *SMM* flares, Share et al. (2002) showed that the measured deexcitation-line Doppler shifts imply interacting-ion angular distributions that are inconsistent with no PAS ($\lambda\rightarrow\infty$), obtaining better fits with values of $\lambda = 300$ or less. Here we assume a level of PAS given by $\lambda = 300$. The atmospheric model is the sunspot model of Avrett (1981), and the accelerated-particle power-law spectral index was assumed to be 4, typical of gamma-ray line flares (Ramaty et al. 1996). We assume a loop length of 1.15×10^9 cm and $\delta = 0.2$, values found by Hua et al. (1989) to provide good fits to deexcitation-line decay times in the 1980 June 21 flare.

For the two threshold energies, 1 and 25 MeV nucleon^{-1}, we show in Figure 10 the fraction of reactions occurring deeper than a given depth in the solar atmosphere, with dashed lines indicating the 50% points. Reactions with a low threshold occur at significantly higher elevations, with a difference in density of more than two orders of magnitude for this model atmosphere. Thus, positron-emitter production from the low-threshold ^{3}He reactions would occur higher in the chromosphere and at lower densities than production from proton and α-particle reactions.

If the temperature of this lower-density region were sufficiently high during the flare, these positrons would add a broad thermal component to the line profile. However, Figure 9 shows that for the July 23 ^{3}He/α upper limit of 0.23, the ^{3}He reactions would only contribute $\sim$30% to the 0.511 MeV line. Even if these positrons annihilated in a high-temperature region, their contribution to the line would not be sufficient to produce a line shape consistent with the width measurement for this flare.

5. SUMMARY

We have shown that accelerated ^{3}He can produce a significant number of positrons in solar flares with steep accelerated-particle spectra, particularly if the ^{3}He/α ratio is $\geq$1, as observed in some impulsive SEP events in interplanetary space. Because of their low threshold energies, these ^{3}He reactions tend to occur at lower densities in the solar atmosphere than the reactions of protons and α-particles. If the temperature at these lower densities is higher than inferred from current atmospheric models, such positrons would add a broad thermal component to the line profile. However, for the 2002 July 23 flare observed by *RHESSI*, the measured 99% confidence upper limit for the ^{3}He/α ratio, 0.23, is probably not sufficient to fully explain the observed line shape for this flare.

A full understanding of the annihilation line will require a comprehensive, self-consistent calculation of annihilation-line production. The calculations must include the transport of the accelerated particles and depth distribution of positron-emitter production, transport of the emitted positrons, and all possible processes by which positrons annihilate (direct annihilation, positronium formation, quenching, etc.). All of these calculations must be performed within the context of a realistic magnetic-loop model assuming various solar atmospheres. This comprehensive study will allow us to construct an annihilation line profile that is composed of contributions from a range of physical conditions determined by the depth distribution of positron production, transport and annihilation. All of the processes involved in the formation of the positron-annihilation line are sensitive to the physical state of the flaring loop such as temperature, density, ionization, and magnetic-field configuration. This line, whose previous

theoretical treatments assumed only simplified conditions, will become an exceptionally sensitive tool for exploring the physical conditions of the solar flare region.

This work was supported by NASA DPR W19,977 and the Office of Naval Research. B. Kozlovsky acknowledges the Israeli Science Foundation for support.

REFERENCES

Anders, E., & Grevesse, N. 1989, Geochim. Cosmochim. Acta, 53, 197
Aschwanden, M. J., Wills, M. J., Hudson, H. S., Kosugi, T., & Schwartz, R. A. 1996, ApJ, 468, 398
Aslanides, E., Fassnacht, P., Dellacasa, G., Gallio, M., & Tuyn, J. W. N. 1981, Phys. Rev. C, 23, 1826
Avrett, C. W. 1981, in The Physics of Sunspots, ed. L. E. Cram & J. H. Thomas (Sunspot: Sacramento Peak National Obs.), 235
Blatt, J. M, & Weisskopf, V. F. 1952, in Theoretical Nuclear Physics (New York: Wiley), 394
Brekke, P., Rottman, G. J., Fontenla, J., & Judge, P. G. 1996, ApJ, 468, 418
Brill, O. D. 1965, Soviet J. Nucl. Phys., 1, 37
Bromley, D. A., & Almqvist, E. 1960, Rep. Prog. Phys., 23, 544
Cochran, D. R. F., & Knight, J. D. 1962, Phys. Rev., 128, 1281
Crandall, W. E., Millburn, G. P., Pyle, R. V., & Birnbaum, W. 1956, Phys. Rev., 101, 329
Fitschen, J., Beckmann, R. Holm, U., & Neurt, H. 1977, Int. J. Appl. Radiat. Isotopes, 28, 781
Frantzvog, D. J., Kunselman, A. R., Wilson, R. L., Zaidins, C. S., & Detraz, C. 1982, Phys. Rev. C, 25, 770
Fuchs, H., & Oeschler, H. 1973, Nucl. Phys. A, 202, 396
Gadioli, E., & Hodgson, P. E. 1986, Rep. Prog. Phys., 49, 951
Geiss, J. 1982, Space Sci. Rev., 33, 201
Hahn, R. L., & Ricci, E. 1966a, Phys. Rev., 146, 650
———. 1967, Nucl. Phys. A, 101, 353
Hazan, J. P., & Blann, M. 1965, Phys. Rev., 137, 1202
Hua, X.-M., Ramaty, R., & Lingenfelter, R. E. 1989, ApJ, 341, 516
Keller, K. A., Lange, J., & Munzel, H. 1974, *Q*-values and Excitation Functions of Nuclear Reactions, Part C, Estimation of Unknown Excitation Functions and Thick Target Yields for p, d, ^{3}He and α Reactions, ed. H. Schopper (Berlin: Springer) (KLM74)
Keller, K. A., Lange, J., Munzel, H., & Pfennig, G. 1973, *Q*-values and Excitation Functions of Nuclear Reactions, Part B, Excitation Functions for Charged Particle Induced Nuclear Reactions, ed. H. Schopper (Berlin: Springer)
Kozlovsky, B., Lingenfelter, R. E., & Ramaty, R. 1987, ApJ, 316, 801
Manzhavidze, N., Ramaty, R., & Kozlovsky, B. 1997, ApJ, 489, L99
———. 1999, ApJ, 518, 918
Michel, R., & Galas, M. 1983, Nucl. Phys. A, 404, 77
Murphy, R. J., Dermer, C. D., & Ramaty, R. 1987, ApJS, 63, 721
Ramaty, R. 1986, in The Physics of the Sun, Vol. 2, ed. P. A. Sturrock (Dordrecht: Reidel), 291
Ramaty, R., Mandzhavidze, N., & Kozlovsky, B. 1996, in AIP Conf. Proc. 374, High Energy Solar Physics, ed. R. Ramaty, N. Mandzhavidze, & X.-M. Hua (New York: AIP), 172
Raymond, J. C., Ciaravella, A., Dobryzka, D., Strachan, L., Ko, Y.-K., & Uzzo, M. 2003, ApJ, 597, 1106
Reames, D. V. 1995, Adv. Space Res., 15 (7), 41
———. 1999, Space Sci. Rev., 90, 413
———. 2000, in ASP Conf. Ser. 206, High Energy Solar Physics: Anticipating HESSI, ed. R. Ramaty & N. Mandzhavidze (San Francisco: ASP), 102
Reames, D. V., Meyer, J.-P., & von Rosenvinge, T. T. 1994, ApJS, 90, 649
Share, G. H., & Murphy, R. J. 1997, ApJ, 485, 409
———. 1998, ApJ, 508, 876
———. 1999, Proc. 26th Int. Cosmic Ray Conf. (Salt Lake City), 6, 13
Share, G. H., Murphy, R. J., Kiener, K., & de Sereville, N. 2002, ApJ, 573, 464
Share, G. H., et al. 2003, ApJ, 595, L85
Smith, D. M., Share, G. H., Murphy, R. J., Schwartz, R. A., Shih, A. Y., & Lin, R. P. 2003, ApJ, 595, L81
Tatischeff, V., et al. 2003, Phys. Rev. C, 86, 025804
Zweibel, E. G., & Haber, D. 1983, ApJ, 264, 648